Automated tape-target centering based on template matching for construction measurement tasks using robotic total stations

Joshua Harrington[1], **Nolan W. Hayes**[1], **and Diana Hun**[1]

[1]Buildings and Transportation Science Division, Oak Ridge National Laboratory, United States of America *

harringtonjd@ornl.gov, hayesnw@ornl.gov, hunde@ornl.gov

Abstract -

Robotic total stations have transformed surveying and construction mapping through precise, efficient, and automated measurements. These instruments integrate a theodolite, which measures horizontal and vertical angles, with an electronic distance measurement (EDM) unit, allowing accurate 3D measurement of observable points. Traditionally, users manually aimed the total station at a target. Recent advancements in robotic motor control and integration of cameras now enable automatic rotation and aiming, typically requiring only a single operator to position the target. Automated aiming is commonly performed using retroreflector prisms, which reflect light back to the source with minimal scattering, enabling high-precision measurements over long distances. However, retroreflectors, especially those designed for 360° visibility, can be expensive and impractical for certain applications. This paper presents an algorithm for automating the center detection of low-cost disposable tape targets using the total station's onboard camera and a template matching algorithm. The algorithm identifies the target's center pixel in the image, and the instrument is commanded to aim at that location. We evaluated the performance of this template-matching-based centering method under various distances, angles, lighting conditions, and field environments, comparing its results to both manual aiming and conventional automated aiming of tape targets. Manual aiming was used as the baseline operational reference in the absence of an independent ground-truth measurement. The proposed approach achieves target centering results comparable to the manual baseline. This method provides a cost-effective alternative for high-precision applications where retroreflector targets are constrained by budget or logistics.

Keywords -

total station, automation, computer vision, template matching

*__Notice__: This manuscript has been authored by UT-Battelle, LLC, under contract DE-AC05-00OR22725 with the US Department of Energy (DOE). The US government retains and the publisher, by accepting the article for publication, acknowledges that the US government retains a nonexclusive, paid-up, irrevocable, worldwide license to publish or reproduce the published form of this manuscript, or allow others to do so, for US government purposes. DOE will provide public access to these results of federally sponsored research in accordance with the DOE Public Access Plan (https://www.energy.gov/doe-public-access-plan).

(a) Robotic total station (b) Retroreflector Prism (c) Tape target

Figure 1. Surveying hardware and targets

1 Introduction

The integration of robotic image-assisted total stations into land surveying and construction mapping represents a significant advancement in geospatial measurement. These instruments have transformed traditional surveying practices by enabling precise, efficient, and largely automated data collection, thereby reducing labor requirements and improving measurement accuracy [1, 2].

Robotic total stations (Fig. 1A) combine three essential components: (1) a theodolite for measuring horizontal and vertical angles, (2) an electronic distance measurement (EDM) unit for determining distances to a target, and (3) an onboard computer that synthesizes angular and distance data to compute three-dimensional coordinates [1]. Traditionally, total stations required manual operation, with surveyors physically aiming the instrument at a target to acquire measurements, a labor-intensive process that often necessitated a two-person crew.

Recent advancements in robotic motor control and automation have enabled these instruments to autonomously rotate, track, and precisely aim at targets, significantly streamlining field operations [2]. This automation allows a single operator to conduct surveys by simply positioning a target, typically a retroreflective prism, while the instrument tracks the target and performs the measurements. Additionally, the integration of cameras onto robotic total stations has added another level of sensing for improved automation; however, the onboard cameras are historically underutilized especially with the advent of advanced computer vision algorithms and image segmentation.

Retroreflective prisms (Fig. 1B) are essential to this system, as they reflect incident light directly back to the source with minimal angular deviation, enabling high-precision distance and angle measurements over long ranges. Among these, 360-degree prisms are particularly valued for their ability to reflect signals from any direction, enhancing flexibility and efficiency in dynamic field environments. However, despite their advantages, such prisms can be prohibitively expensive and may not be suitable for all applications, especially in cost-sensitive or temporary deployments.

As a lower-cost alternative, disposable tape targets (Fig. 1C) are often used. These targets are inexpensive, easy to deploy, and can be left in place without concern for recovery. However, current methods for automating the centering of the total station's telescope on these targets often result in reduced accuracy. Consequently, users must manually aim the telescope at the center of each target to ensure reliable measurements, reintroducing inefficiencies in labor and time.

Surveying with total stations to evaluate the placement accuracy (tolerances) of building components is common practice. For example, surveys crews often manually aim at installed wall panels to confirm they fall within the required tolerances. In some cases, particularly for challenging installations, a crew may even take measurements in-process and guide crane operations in real time to ensure components are positioned correctly. Recent research has investigated automated measurement systems that use a total station to guide crane placement of building components [3, 4]. In these systems, retroreflector targets are attached to building components enabling automated measurements of installation error in real time and providing guidance during placement. However, these retroreflector targets must be manually retrieved after installation. A more effective alternative is to enable automated, precise measurement of disposable targets. Such targets could be left in place, either falling off naturally over time or being removed later, eliminating the need for retrieval during installation.

This paper presents a novel workflow for automating the detection of and centering on low-cost disposable tape targets using the total station's onboard camera and a template matching algorithm. The proposed method identifies the center pixel of the target in the captured image and commands the instrument to aim accordingly. We evaluate the performance of this template-matching-based centering approach under a range of distances, angles, lighting conditions, and field scenarios, comparing its accuracy to both manual aiming and conventional automated methods for tape targets. This approach offers a cost-effective alternative for high-precision applications where the use of retroreflectors is limited by budget or logistical constraints.

1.1 Literature Review

Research focused on automating the precise measurement of tape targets remains limited. Schwieger, Kerekes, and Lerke explored methods for detecting object features using the onboard camera of a total station [1]. However, their approach still relied on active measurement using a retroreflective prism to determine precise object positions.

Zschiesche and Schlüter [5] investigated potential applications of machine learning and image segmentation in image-assisted total stations. Their work focused on identifying various types of targets, including reflectorless ones, within images captured by the various cameras of the total station. However, they did not explore methods to automate the precise centering of the telescope on these targets.

Lian et al. [6] developed a machine vision-based approach for automating the aiming process at tape targets using template matching. While promising, their method achieved peak accuracy of approximately 5 millimeters at distances of 70 meters and 131 meters.

The method proposed in this paper builds upon Lian et al.'s work, aiming to demonstrate improved accuracy at medium ranges up to 100 meters. Sub-3-millimeter accuracy is needed to meet tolerance requirements for typical building component installation such as precast concrete or steel structure [7, 8]. For these construction tasks, tolerances can be as low as 3 millimeters. The proposed method improves the template matching algorithm to achieve sub-3.3-mm accuracy up to 100 meters.

2 Methodology

2.1 Multi-Scale Template Matching

Automated aiming is performed using a multi-scale template matching pipeline consisting of (1) image capture, (2) green-channel extraction, (3) Gaussian blurring, (4) multi-scale template matching, and (5) telescope pointing.

The template was approximated in code rather than photographed under a single condition. Feature shapes, colors, and relative sizes were iteratively tuned using a diverse set of sample images to ensure robust matching across the range of conditions evaluated. Exact proportional replication was unnecessary for accurate matching since the apparent template shape varies with viewing angle.

Two template versions were developed. The first included only the center black cross on a white rectangular background. The second included concentric gray circles (intensity = 100) on a similar background. Feature sizes were visually tuned to match their appearance at distances between 10–130 m. Since the template shape distorts at oblique angles, exact proportional replication was not required for reliable matching.

These templates, shown in Fig. 2 prior to preprocessing, were lightly blurred (Gaussian kernel size = 3, σ = 1.0). Testing with approximately fifteen representative images showed that matching consistently failed at long distances ($\geq$ 70 m) without template blurring.

High-resolution (2560x1920) telescopic color images were captured and transferred via USB to a remote laptop. The green channel was extracted to improve feature contrast, as most camera sensors are optimized for green light. This step improved template matching under low-light conditions and allowed a successful match at 100 m. The images were then lightly blurred with the same Gaussian parameters used for the templates, allowing the pipeline to correctly match more templates from the dataset at larger distances (> 70 m).

To enable matching across a range of distances, the templates were scaled over representative size ranges. For each scaled template, the OpenCV template matching algorithm [9] computed the best score and corresponding pixel location. This process was performed with the first template (cross-only) for 4 scales (1.0-1.3). If the maximum correlation score across the evaluated scales exceeded 0.7, the second template was skipped.

The correlation threshold (0.7) was empirically selected by evaluating a varied test set and choosing the lowest value that consistently produced correct matches across all test cases.

If the maximum correlation score from the first template did not exceed the threshold, the second template was applied across 18 scales (0.3-1.3). These scale ranges were determined by comparing template size to the apparent size of the target in the closest and furthest images (10–130 m for the circular template; 10–40 m for the cross template, which becomes too small to match reliably at longer distances).

Fig. 3 shows an example of the detected template and center pixel. The total station was then aligned with this pixel location using its built-in turn-to-pixel function.

Matching accuracy degraded quickly when using the circular template under oblique viewing angles, as the circles appear elliptical. In contrast, the smaller cross exhibited less geometric distortion at high angles, enabling successful matching at angles up to 50° with a maximum error of 0.3 mm.

2.2 Experiments

A series of experiments were conducted to evaluate the accuracy of the proposed centering algorithm compared to manual aiming and the existing automated centering method. All tests were performed using a consistent set of hardware and a standardized experiment methodology.

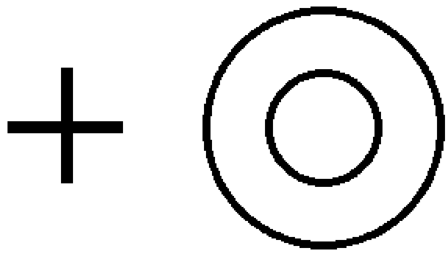

Figure 2. Illustration of templates

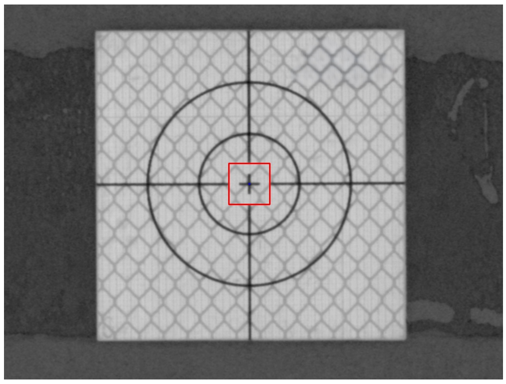

Figure 3. Template matching in telescope camera

2.2.1 Hardware

The experiments utilized a Leica MS60 robotic total station, operated via the GeoCOM protocol through a custom Python interface [10]. This unit features a 5-megapixel telescope camera.

Tape targets manufactured by Leica, measuring 60 mm by 60 mm, were used throughout the tests. A tape target was mounted on a mock brick wall assembly measuring 80 cm by 80 cm. Since several smaller tape targets were also mounted on the wall, covering these targets with pieces of paper was required to prevent either algorithm from finding different targets. This assembly was affixed to an adjustable arm configuration, allowing placement at various angles.

For indoor tests, a synthetic light source was used to control illumination, and a lux meter was employed to measure lighting conditions for each test case. The indoor tests were performed at a light level of 85 lux, and the outdoor tests were done on a partly sunny day with an average illuminance of 5000 lux.

2.2.2 Experiment Workflow

Experiment for Proof-of-Concept. The experimental workflow was designed to generate baseline comparisons and assess the accuracy of both the existing and proposed centering methods. Each test followed the steps below:

1. **Manual Aiming:** The total station was manually aligned with the center of the tape target. Five rapid distance measurements were collected and averaged to reduce EDM readout jitter.

2. **Existing Method:** The instrument was rotated to a random vertical and horizontal offset (within limits to ensure it remained visible). The existing method was executed and five distance measurements were averaged. Because of noticeable run-to-run variability, this procedure was repeated three times per setup (Sec. 4.1).

3. **Proposed Method:** A telescope image was captured, downloaded to the remote computer, and processed using the multi-scale template matching algorithm. The computed center pixel was used to re-aim the instrument using a builtin turn-to-pixel function. The algorithm was run only once per setup because little variability had been observed previously (Sec. 4.1). Finally, five distance measurements were averaged.

The existing automated centering method is proprietary, and its internal operation is undisclosed. Based on observable behavior, the method appears to use a flashing guide light, detecting and centering on the reflected shape of the tape target, similar to the procedure used for retroreflective prisms.

The experimental workflow was repeated across a predefined combination of viewing angles, distances, and lighting conditions. Table 1 summarizes the experimental setups. Set A varied horizontal viewing angle at a fixed 10 m distance (0°–60°), and Set B varied distance from 10–130 m under near-normal incidence. For each setup, telescope images were also recorded for qualitative comparison.

Template matching performance depends on both image resolution and the target distance. Lighting conditions also affect the matching accuracy. Some tests were performed indoors at shorter distances and under low light conditions, while longer range tests were done outdoors. The distance range of 10 - 130 m targeted medium-range applications (precise measurement of component locations with attached tape targets [3, 4]), while also identifying the upper slope distance limit given the available hardware.

Another factor influencing algorithm performance is the skew of the target within the image relative to the template. At extreme viewing angles, the algorithm may struggle to match the tape target accurately. To assess angular robustness, the tape target was rotated horizontally relative to its surface normal (0°), as illustrated in Fig. 4. The horizontal viewing angle, H, was varied from 0° to 60°. Because the tape target is symmetric, only one rotation direction was assessed.

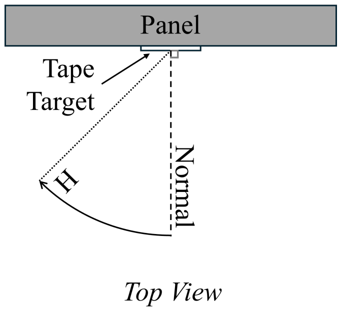

Figure 4. Illustration of horizontal viewing angle

Illumination was controlled to represent low light indoors (85 lux) and bright outdoor daylight (5000 lux). Higher illuminance levels are expected to enhance algorithm performance by improving image clarity and contrast.

Experiment for Statistical Analysis. A separate experiment evaluated run-to-run variability in the error across each algorithm. Manual centering was performed initially as before using Setup A1 (Table 1). The instrument was given a programmed random angular nudge within predefined limits before each run. The existing method was repeated 20 times and the average of 5 distance measurements was recorded for each run. The procedure was repeated for the proposed method to allow a direct comparison.

3 Results

The experimental results compare tape target centering performance across the three methods evaluated: manual aiming, the existing onboard centering method, and the proposed template matching centering method.

For each test, telescope camera images were captured at three stages: (1) after manual aiming, (2) after centering using the existing method, and (3) after centering using the proposed template matching method.

A representative subset of images from five tests is shown in Fig. 5. For each condition, the figure shows the following:

- **Manual Method**: crosshair placement after manual alignment.

- **Existing Method**: the median-error result from the three onboard centering attempts.

- **Proposed Method**: crosshair placement after executing the proposed method.

These visual comparisons illustrate how the proposed method tends to produce centering results that are closer to

Table 1. Experiment conditions and setups

Test No.	Conditions			
	Location	Target Distance (m)	Viewing Angle, H (°)	Illumination
Set A				
A1	Indoor	10	0	Low
A2	Indoor	10	10	Low
A3	Indoor	10	20	Low
A4	Indoor	10	30	Low
A5	Indoor	10	40	Low
A6	Indoor	10	50	Low
A7	Indoor	10	60	Low
Set B				
B1	Outdoor	10	0	High
B2	Outdoor	20	0	High
B3	Outdoor	30	0	High
B4	Outdoor	40	0	High
B5	Outdoor	70	0	High
B6	Outdoor	100	0	High
B7	Outdoor	130	0	High

the apparent target center under the conditions shown. A brief quantitative analysis of error variability is provided in Sec.4.1.

To verify that averaging five sequential readings sufficiently suppresses readout jitter, we examined within-run dispersion under representative conditions. For example, for Setup A4 (existing method, run 3), the five readings yielded a mean error of 0.03 mm with a standard deviation of 0.03 mm, indicating negligible short-term variability. Comparable levels were observed across other runs; therefore, we report per-run averages for all experiments.

Fig. 6 records the mean, minimum, and maximum error for the existing method and the corresponding error in the proposed method. As described in Sec. 4.1, the existing method exhibited substantial run-to-run variability, whereas the proposed method did not. Consequently, the proposed method was executed once per setup, with its design choice validated by the variability analysis.

Entries marked "Algorithm Failed" indicate conditions in which the method did not identify the target in any run (0% detection success). In all successful cases, the method identified the target in every run (100% success).

Manual aiming provided the baseline for computing errors. Since no ground-truth reference was available, these values represent only a relative reference. The errors reported for the existing and proposed methods are Euclidean distances between the method-measured positions and the corresponding manual measurement. These representative errors are reported in Fig. 6.

4 Discussion

The user manually aligned the crosshairs with the tape target center using the telescope view. As shown in Fig. 5, the manual method exhibited visually consistent target alignment. However, manual centering is inherently subjective and sensitive, particularly at long slope distances, where wind-induced vibrations, reduced image quality, and temperature gradients further decrease accuracy. A single user performed all manual aiming tasks to minimize variability in the baseline measurements. Although this introduces potential operator-specific bias, maintaining consistency in the manual reference measurements was prioritized.

Visual inspection of the existing method in Fig. 5 combined with the calculated errors in Fig. 6 indicates significant variability. Particularly at longer distances or angles, the onboard proprietary algorithm struggled to center on the target, frequently leading to variable and inaccurate results.

The largest mean error observed for the existing method was 8.5 mm, and the mean errors across all experimental setups had an overall average of 4.9 mm (see individual means in Fig. 6). These values exceed many common construction installation tolerances, some of which are as small as 3 mm [7, 8].

At target slope distances above approximately 30 m, the existing method fails to identify the target in all trials (0% detection or measurement success).

The proposed method demonstrated lower centering error than the existing method under all successful trials, achieving a maximum deviation of 3.3 mm from the baseline. Within 70 m, the deviation decreased to less than 1 mm. Although performance declines at extreme distances and angles, the algorithm consistently outperformed the existing method across all tested scenarios.

Although the primary goal of this investigation was to develop a method for accurate automated measurement of tape targets at intermediate distances (20 to 40 m), testing extended until failure occurred at a slope distance of 130

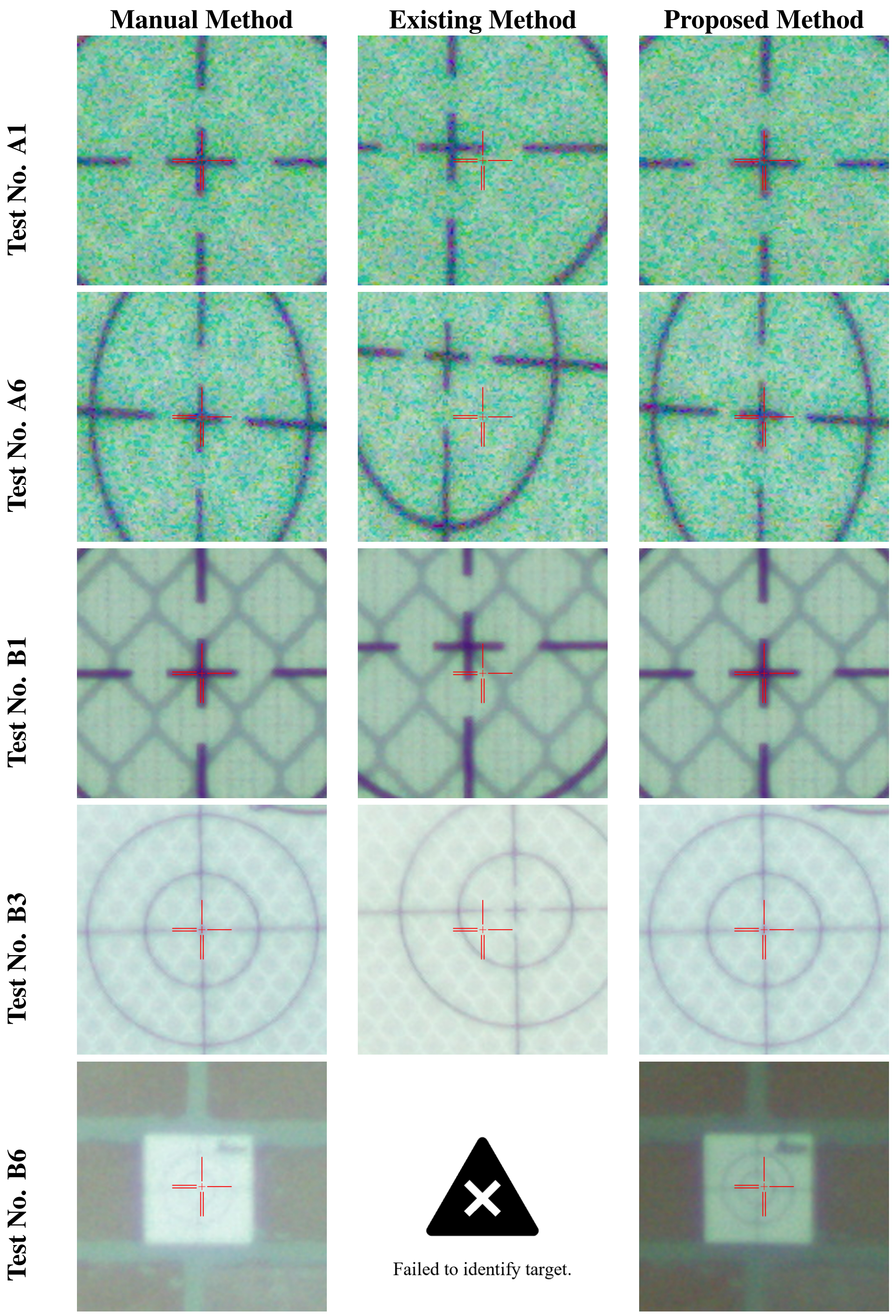

Figure 5. Representative telescope images of aiming methods for multiple test conditions

m, substantially beyond the onboard method's limit of 40 m. The cause of failure at this distance is not yet clear, as image statistics and background conditions were comparable to those in successful trials. Additional investigation will be needed to determine the specific factors governing long-range performance.

4.1 Statistical Analysis of Measurement Error

In addition to the proof-of-concept experiments, a statistical analysis was performed to quantify measurement variability and validate the experimental design. Two primary variability sources were considered for the proposed method: (1) small differences in the captured images and (2) the onboard turn-to-pixel function. Despite these factors, the proposed method exhibited low variability compared to the existing method (Fig. 7). In Setup A1, the

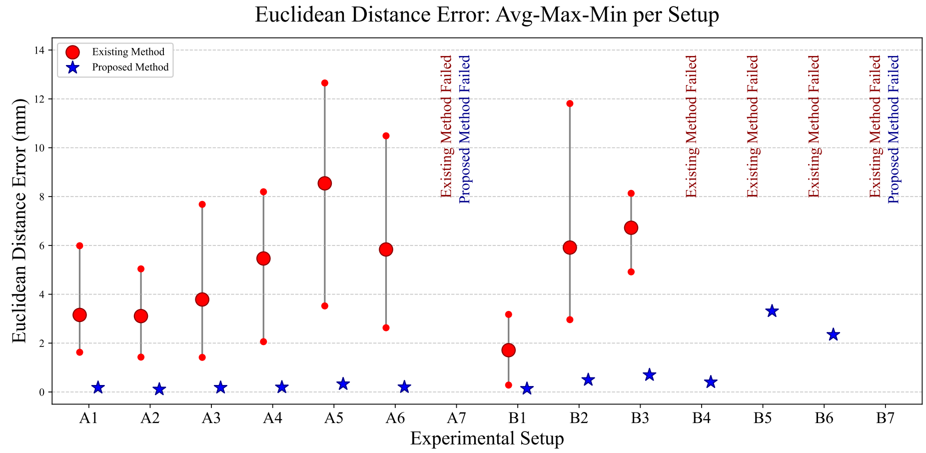

Figure 6. Avg-max-min Euclidean distance error per experimental setup.

existing method produced a mean error of 5.2 mm with a standard deviation of 3.1 mm (95% CI: ±1.5 mm), whereas the proposed method produced a mean error of 0.16 mm with a standard deviation of 0.04 mm (95% CI: ±0.02 mm).

4.2 Limitations

The proposed template-matching algorithm requires the full tape target to be visible within the telescope camera's field of view. During testing, the existing method provided this initial coarse alignment; therefore, the current implementation of the proposed algorithm is not yet fully autonomous. A fully autonomous workflow could incorporate image-segmentation techniques to coarsely align the target before precisely centering with template matching.

A second limitation is the 10–20 s required to download a telescope image from the instrument to the remote computer. This delay is specific to the instrument used in testing and dominates the cycle time, preventing real-time tracking of moving targets. The image-processing stage itself requires only about 0.5 s and could be further optimized for tracking. Eliminating the download time by real-time video streaming or running the proposed method directly onboard the instrument would allow the method to be competitive with manual operation times and track targets in real-time.

5 Conclusions

A template-matching algorithm was developed to automate the centering of a robotic total station on disposable tape targets. The method was evaluated across a range of distances, angles, and lighting conditions. Within the tested envelope, the algorithm achieved centering performance comparable to manual centering for viewing angles up to 50° and distances from 10-100 m. Since no independent ground-truth reference was available, all reported errors represent deviations from the manual baseline.

The current implementation is not fully autonomous, since the template must be positioned within the camera's field of view. Additionally, overall cycle time is dominated by instrument-specific image-transfer delays rather than by algorithmic processing. Eliminating this bottleneck with a live video stream or through onboard execution would allow real-time performance.

Quantitatively, the proposed algorithm increased the usable range from less than 40 m (existing method) to 10–100 m, and reduced the overall average centering error (relative to the manual baseline) from 4.9 mm to 0.7 mm. These results demonstrate that the proposed method provides a cost-effective and substantially more accurate alternative for high-precision applications where retroreflectors are impractical.

5.1 Future Research

Future research will extend the tape centering algorithm to dynamic scenarios, including real-time target tracking. This will require optimizing the algorithm's processing time, improving its robustness in challenging lighting and viewing conditions, and eliminating the image-transfer latency. Additional work will explore integration with higher-resolution imaging systems and the development of a fully autonomous pipeline that does not require coarse alignment with the onboard method.

6 Acknowledgments

This material is based upon work supported by the U.S. Department of Energy, Office of Critical Minerals and En-

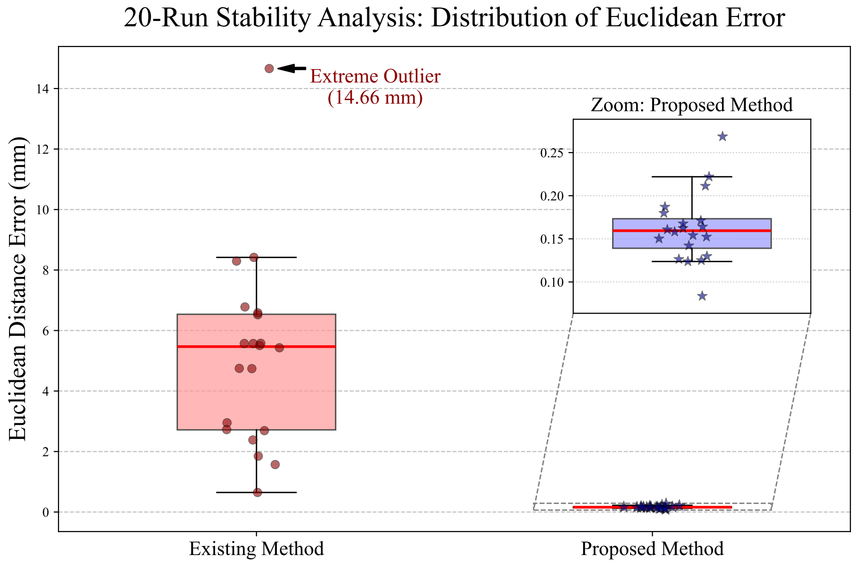

Figure 7. Box-and-whisker plot for 20-run statistical analysis of Setup A1.

ergy Innovation (CMEI), specifically the Building Technologies Office under contract DE-AC05-00OR22725.

The views expressed herein do not necessarily represent the views of the U.S. Department of Energy or the United States Government.

6.1 Notice of Copyright

This manuscript has been authored [optional: in part] by UT-Battelle, LLC, under contract DE-AC05-00OR22725 with the US Department of Energy (DOE). The US government retains and the publisher, by accepting the work for publication, acknowledges that the US government retains a non-exclusive, paid-up, irrevocable, world-wide license to publish or reproduce the submitted manuscript version of this work, or allow others to do so, for US government purposes. DOE will provide public access to these results of federally sponsored research in accordance with the DOE Public Access Plan (https://energy.gov/doe-public-access-plan).

6.2 Declaration of generative AI and AI-assisted technologies in the manuscript preparation process

During the preparation of this work, the authors used Copilot in order to improve manuscript clarity, conciseness, and grammar. After using this tool, the authors reviewed and edited the content as needed and take full responsibility for the content of the published paper.

References

[1] Volker Schwieger, Gabriel Kerekes, and Otto Lerke. *Image-Based Target Detection and Tracking Using Image-Assisted Robotic Total Stations*, pages 133–169. Springer International Publishing, Cham, 2020. ISBN 978-3-030-22587-2. doi:10.1007/978-3-030-22587-2_5. URL `https://doi.org/10.1007/978-3-030-22587-2_5`.

[2] Fernando Reyes-Aviles, Thomas Gloor, and Clemens Arth. Automatic model-based stationing: Robust total station localization without known control points. *J. Intell. Robot. Syst.*, 111(1), March 2025.

[3] Nolan W. Hayes, Bryan P. Maldonado, Diana Hun, and Peter Wang. Real-time evaluator to optimize and automate crane installation of prefabricated components. In *Proceedings of the 40th International Symposium on Automation and Robotics in Construction*, pages 192–199, Chennai, India, July 2023. International Association for Automation and Robotics in Construction (IAARC). ISBN 978-0-6458322-0-4. doi:10.22260/ISARC2023/0028.

[4] Nolan W Hayes, Bryan P Maldonado, Mengjia Tang, Peter Wang, and Diana Hun. Optimization of prefabricated component installation using a real-time evaluator (RTE) connection locating system. In *Proceedings of the 41st International Symposium on Automation and Robotics in Construction*, pages 65–72, Lille, France, June 2024. International Association for Automation and Robotics in Construction (IAARC). ISBN 978-0-6458322-1-1. doi:10.22260/ISARC2024/0010.

[5] Kira Zschiesche and Martin Schlüter. Classification and object detection with image assisted total station and machine learning. *Journal of Applied Geodesy*, 17(4):381–389, 2023. doi:doi:10.1515/jag-2023-0011. URL `https://doi.org/10.1515/jag-2023-0011`.

[6] Hou Lian, Zhao Long-fei, Zeng Wei, Yang Lei, and Xiao Changshi. Research on fully automatic template calibration method based on machine vision guidance. *China Rural Water and Hydropower*, pages 185–192, December 2024. doi:10.12396/znsd.232026.

[7] Precast/Prestressed Concrete Institute. PCI 135-25: Specification for Tolerances of Precast Concrete. Standard, 2025.

[8] American Institute of Steel Construction. Specification for structural steel buildings. AISC 360-22, 2022.

[9] G. Bradski. The OpenCV Library. *Dr. Dobb's Journal of Software Tools*, 2000.

[10] MrClock8163. GeoComPy. `https://github.com/MrClock8163/geocompy`, 2025.